

University of Groningen

Evidence of upper-critical-field enhancement in K3C60 powders

Boebinger, G.S.; Palstra, T.T.M.; Passner, A.; Rosseinsky, M.J.; Murphy, D.W.

Published in:
Physical Review B

DOI:
[10.1103/PhysRevB.46.5876](https://doi.org/10.1103/PhysRevB.46.5876)

IMPORTANT NOTE: You are advised to consult the publisher's version (publisher's PDF) if you wish to cite from it. Please check the document version below.

Document Version
Publisher's PDF, also known as Version of record

Publication date:
1992

[Link to publication in University of Groningen/UMCG research database](#)

Citation for published version (APA):

Boebinger, G. S., Palstra, T. T. M., Passner, A., Rosseinsky, M. J., & Murphy, D. W. (1992). Evidence of upper-critical-field enhancement in K3C60 powders. *Physical Review B*, 46(9).
<https://doi.org/10.1103/PhysRevB.46.5876>

Copyright

Other than for strictly personal use, it is not permitted to download or to forward/distribute the text or part of it without the consent of the author(s) and/or copyright holder(s), unless the work is under an open content license (like Creative Commons).

The publication may also be distributed here under the terms of Article 25fa of the Dutch Copyright Act, indicated by the "Taverne" license. More information can be found on the University of Groningen website: <https://www.rug.nl/library/open-access/self-archiving-pure/taverne-amendment>.

Take-down policy

If you believe that this document breaches copyright please contact us providing details, and we will remove access to the work immediately and investigate your claim.

Downloaded from the University of Groningen/UMCG research database (Pure): <http://www.rug.nl/research/portal>. For technical reasons the number of authors shown on this cover page is limited to 10 maximum.

Evidence of upper-critical-field enhancement in K_3C_{60} powders

G. S. Boebinger, T. T. M. Palstra, A. Passner, M. J. Rosseinsky, and D. W. Murphy
AT&T Bell Laboratories, Murray Hill, New Jersey 07974

I. I. Mazin*

Max Planck Institut für Festkörperforschung, 7000 Stuttgart 80, Germany
 (Received 1 April 1992; revised manuscript received 29 May 1992)

ac susceptibility measurements of superconducting K_3C_{60} powders in magnetic fields to 30 T yield a roughly linear $H_{c2}(T)$ curve extending up to the highest experimental fields. Samples prepared by two different methods give $-dH_{c2}/dT = 2.14 \pm 0.08$ T/K, with $T_c = 18.7$ K. The observed H_{c2} at low temperatures exceeds the $H_{c2}(T)$ curve from the standard theory by Werthamer-Helfand-Hohenberg. We discuss the role of flux motion and evidence for enhancement of H_{c2} by intrinsic mechanisms such as strong coupling, Fermi surface anisotropy, and/or granularity of the samples.

Superconductivity in alkali-metal fullerenes¹ has yielded high transition temperatures accompanied by very high values for $-dH_{c2}/dT$ near T_c . Extrapolations from low-magnetic-field data yield estimated magnitudes of the upper critical field, $H_{c2}(T=0)$, ranging as large as ~ 50 T.²⁻⁵ Pair breaking due to high magnetic fields occurs roughly when one flux quantum threads each coherence area of an electron pair: $H_{c2} = \Phi_0/2\pi\xi_{GL}^2$, where ξ_{GL} is the Ginzburg-Landau coherence length. Thus, measurement of upper-critical magnetic fields directly determines the Ginzburg-Landau coherence length. Within the traditional picture of phonon-mediated superconductivity, $\xi_{GL} = \xi_0$ in the clean limit, where ξ_0 is the Pippard coherence length. In the dirty limit, $\xi_{GL} \sim (\xi_0 l_{mfp})^{1/2}$, where l_{mfp} is a mean free path, which could originate from microscopic disorder or sample granularity. Thus, in C_{60} -based superconductors, high upper critical fields might result in part from an orientational disorder between adjacent C_{60} molecules, which limits l_{mfp} .⁶ Additional enhancements of the upper critical field at low temperatures could result from strong electron-phonon coupling, as has been proposed to result from the supersoft rotational phonons among neighboring C_{60} molecules.⁷ Fermi-surface anisotropy can also provide low-temperature enhancement of the upper critical field. All of these mechanisms will be discussed later in conjunction with our high-field data.

In both clean- and dirty-limit BCS theory, a high upper critical field often is the result of a small electron bandwidth because ξ_0 is proportional to the Fermi velocity, which should decrease as the electron bandwidth decreases. Thus, one expects high H_{c2} values for narrow d - and f -band metals, such as the A15, Chevrel, and heavy-electron compounds. In contrast, s - and p -band metals like Al or In contain sufficiently wide bands that the critical fields are of order 10^{-2} T. In alkali-metal intercalated C_{60} , the energy bands near the Fermi energy originate mainly from carbon p orbitals; however, the weak coupling between individual molecules results in a band structure characterized by only slightly broadened molec-

ular orbitals. Indeed, band-structure calculations of K_3C_{60} indicate that the conduction band derived from half-filled t_{1u} orbitals has a width of only ~ 0.6 eV.^{8,9} In conjunction with the high phonon frequencies associated with the electron-phonon coupling,¹⁰⁻¹⁴ such narrow bands would imply that K_3C_{60} violates Migdal's theorem, which states that the Fermi energy should be much larger than the phonon frequencies for BCS-like behavior. Thus, even if the superconductivity in K_3C_{60} is phonon mediated, the upper critical field might exhibit anomalous behavior. The role of Coulomb interactions in a system with narrow, molecularlike bands is not yet clear either. It has been claimed that such narrow bands do not allow sufficient renormalization of the Coulomb repulsion for the repulsion to be overcome by a phonon-mediated attraction,¹⁵ and a correlation-induced superconductivity has been proposed.¹⁶ On the other hand, it can be argued that the relevant bandwidth is the full π band ($\gtrsim 10$ eV), which would strongly renormalize the Coulomb repulsion.^{17,18}

In order to explore the origin of the high upper critical fields, we have measured the upper critical field of K_3C_{60} in magnetic fields up to 30 T. We compare the temperature dependence of H_{c2} to the standard theory by Werthamer-Helfand-Hohenberg (WHH).¹⁹ WHH theory predicts a roughly parabolic $H_{c2}(T)$ curve, which differs only slightly between the clean and dirty limit, when plotted in reduced units $t = T/T_c$ and $h_{c2} = H_{c2}/(-dH_{c2}/dt)_{t=1}$. In contrast, the K_3C_{60} data exhibit deviations from WHH, especially at low temperatures, where measured H_{c2} values exceed the WHH curve determined by fitting the low-field data. Within the traditional model of phonon-mediated superconductivity, such deviations could result from strong coupling, Fermi-surface anisotropy, and/or granularity. Some of the observed deviation from WHH we attribute to the presence of flux motion, which we observe in these samples.

The two samples studied were prepared by different techniques. For each sample, C_{60} powder was extracted from soot and separated from higher fullerenes by

chromatography.²⁰ Potassium intercalation was accomplished either by reacting stoichiometric quantities of C_{60} with pure potassium (sample 1) or KBH_4 (sample 2) in a sealed Pyrex ampoule for several days at temperatures up to 350°C . Samples 1 and 2 are of nominal composition $K_{2.5}C_{60}$ and K_3C_{60} , respectively. X-ray powder diffraction and ^{13}C NMR show that sample 1 is phase separated into K_3C_{60} and (nonsuperconducting) C_{60} , while sample 2 is single-phase K_3C_{60} .²¹ Sample 2 exhibits 23% dc diamagnetic shielding (flux exclusion).²² We expect both samples to exhibit the ac susceptibility of superconducting K_3C_{60} .

The upper critical fields were measured by ac susceptibility using a driving field amplitude of 2 Oe at a frequency of 4 kHz. dc magnetic fields up to 15 T were generated by a superconducting magnet and up to 30 T by the hybrid magnet of the Francis Bitter National Magnet Laboratory at Massachusetts Institute of Technology. The 4-kHz driving frequency was chosen to exceed vibration and magnetic-field noise frequencies of the Bitter magnet. For each datum, the temperature was stabilized and measured using a calibrated carbon-glass thermometer, including corrections for the magnetoresistance measured in the high-dc fields. No evidence of thermal non-equilibrium results from reversing direction of the temperature sweep or from reducing the ac driving field amplitude by three orders of magnitude.

The two panels of Fig. 1 show the temperature dependence of the real part of the ac susceptibility for the mixed phase sample (sample 1) in various applied dc fields. Note that the upper panel contains a tenfold vertical expansion of the data. The data at all fields exhibit a sharp onset for the superconducting transition. The imaginary part of the ac susceptibility exhibits a dissipa-

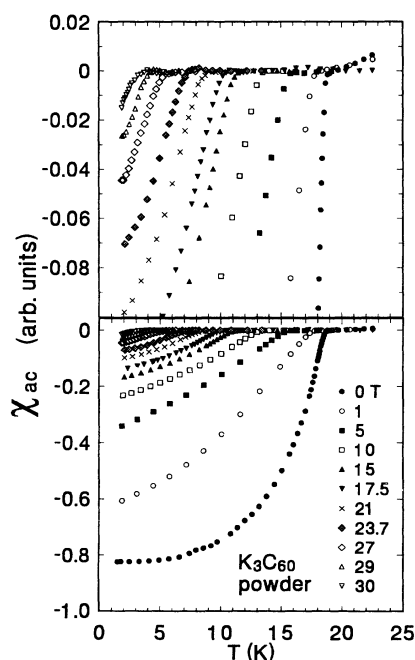


FIG. 1. Real part of the ac susceptibility in arbitrary units of K_3C_{60} powder (sample 1) in dc magnetic fields to 30 T. Note the vertical expansion in the upper panel.

tion peak just below the onset temperature. We define the onset temperature, T_0 , by the intersection of two lines fitted to the data immediately above and below the onset of the transition. Below T_0 , the transition to a low-temperature shielding state is quite broadened. Only the 0-T data exhibit a fully completed transition above 1.4 K. With increasing dc field, T_0 decreases from 18.7 ± 0.1 K at 0 T to 3.1 ± 0.2 K at 30 T. Note that the suppression of T_0 is accompanied by a dramatic decrease in the magnitude of the low-temperature response.

Figure 2 contains these same measurements on the single-phase sample (sample 2). The results are comparable to those from sample 1. The only substantial difference occurs at low temperatures, where the magnetic response is now nearly temperature independent at all magnetic fields, evidencing a fully realized low-temperature shielding state. Note that the vertical axis is scaled in the shielding volume fraction and the 4-kHz ac diamagnetic shielding is $\sim 32\%$ at $H=0$, in reasonable agreement with the dc value. Note also that the low-temperature shielding volume at 30 T is 80 times smaller than the zero-field shielding volume.

The magnetic-field dependence of the transition onset temperature T_0 is shown in Fig. 3 for both samples. The data for the two samples define a common curve accurately characterized by a linear temperature dependence with a slope of 2.14 ± 0.08 T/K, even up to the highest experimental magnetic fields. If we identify T_0 as the superconducting transition temperature T_c , then Fig. 3 represents the upper-critical-field curve for K_3C_{60} . In contrast to the data of Fig. 3, WHH theory yields a roughly parabolic $H_{c2}(T)$ curve, which approaches zero temperature with zero slope at a maximum critical field value of $h_{c2}(T=0) \sim 0.7$, where h_{c2} is the reduced upper critical field defined previously. The solid line in Fig. 3

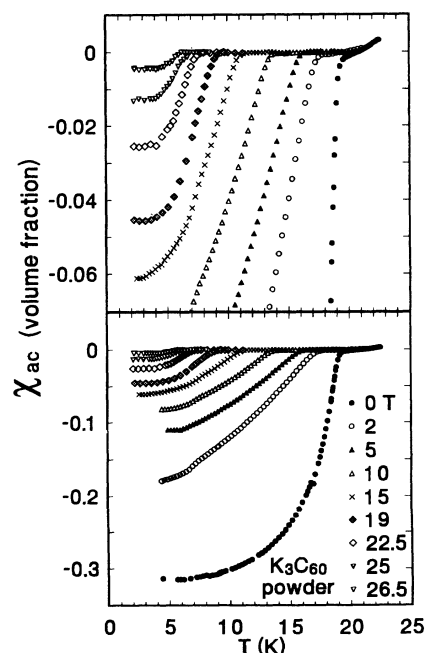


FIG. 2. Real part of the ac susceptibility of K_3C_{60} powder (sample 2) in units of volume fraction (-1 is perfect screening).

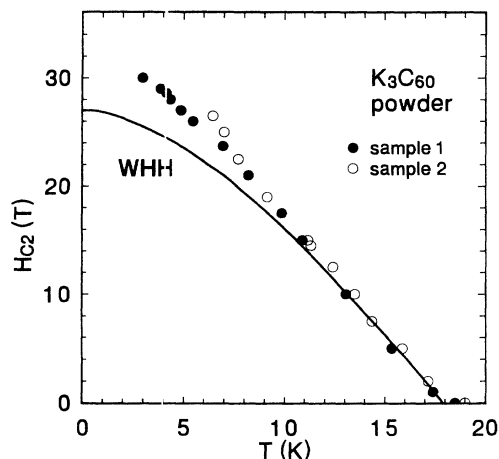


FIG. 3. Onset temperature T_0 vs magnetic field for both samples. The solid line represents the WHH curve fitted to the magnetic field data below 12 T.

represents a WHH curve fitted to the data below 12 T. On the other hand, the roughly linear behavior of the $H_{c2}(T)$ data suggests $h_{c2} \sim 1$ and substantial enhancements of $H_{c2}(0)$ over the WHH theory in K_3C_{60} powders.

The WHH theory is based on a solution of the linearized Gor'kov equations and, therefore, is valid in the weak-coupling regime for materials with isotropic Fermi surfaces. There are a number of intrinsic mechanisms within standard phonon-mediated superconductivity that result in low-temperature deviations from the WHH curve given in Fig. 3: (1) *Spin-orbit coupling*. Energy bands arising from an element as light as carbon will exhibit negligible spin-orbit effects. This is verified by the observation of narrow electron-spin-resonance absorption lines corresponding to an essentially free-electron g factor of 2.00.²³ (2) *Spin paramagnetism*. The paramagnetic limit corresponds to the magnetic field, which breaks Cooper pairs by aligning electron spins. In experimental units of T and K, paramagnetic limiting will become important for magnetic fields exceeding $\sim 1.84 \times T_c \sim 33$ T. Although the Fig. 3 data approach this regime, spin paramagnetism will suppress the upper critical field¹⁹ and, thus, cannot account for the observed enhancement. (3) *Mean-free-path effects*. From $H_{c2} = \Phi_0 / 2\pi \xi_{GL}^2$ and an extrapolated $H_{c2}(0) \sim 30$ –38 T, we deduce a Ginzburg-Landau coherence length, $\xi_{GL} \sim 29$ –33 Å. It is currently unknown whether superconductivity in K_3C_{60} is in the clean limit ($\xi_0 \sim 30$ Å) or dirty limit ($\xi_0 \sim 130$ Å, which assumes l_{mfp} is determined by the diameter of the C_{60} molecule) or somewhere in between. Nonetheless, in moving from the dirty to the clean limit, WHH theory gives only a modest enhancement of $h_{c2}(0)$ from 0.69 to 0.73, where h_{c2} is the reduced upper critical field defined previously. We therefore reject each of these first three mechanisms as inadequate to account for the observed low-temperature enhancement of the upper critical field.

The three remaining mechanisms are possible candidates, though they remain difficult to evaluate quantitatively: (4) *Strong coupling* ($2\Delta > 3.5k_B T_c$). The question of the coupling strength in K_3C_{60} is not yet settled. Mea-

surements of the energy gap from nuclear magnetic resonance²⁴ find $2\Delta/k_B T_c \sim 3.0$, while point-contact tunneling²⁵ gives $2\Delta/k_B T_c \sim 5.3$. Strong-coupling effects can yield a relatively large enhancement of $h_{c2}(0)$, such that the temperature dependence of h_{c2} becomes roughly linear or even superlinear.²⁶ This enhancement is weaker in a dirty superconductor. (5) *Fermi-surface anisotropy*. In the presence of Fermi-surface anisotropy, Hohenberg and Werthamer²⁷ find the renormalization of h_{c2} from the isotropic value is $\langle v_F^2 \rangle / \exp(\langle \ln v_F^2 \rangle)$ in the clean limit. The Fermi surface of K_3C_{60} is known to be very anisotropic.⁸ We have calculated $h_{c2}(0)$ in the three molecular orbital model of Satpathy *et al.*⁹ for two different orientationally ordered C_{60} structures and find an enhancement comparable to our data [$h_{c2}(0) \sim 1$]. However, in the dirty limit, this enhancement would be substantially reduced. (6) *Granularity*. Thin films of K_3C_{60} have been found to be granular on the length scale of the coherence length, as evidenced by transport measurements.^{3,28} In these K_3C_{60} powders, the observed suppression of the magnetic response in high dc fields (Figs. 1 and 2) evidences granularity on the length scale of the penetration depth (microns). However, in granular materials, the upper critical field will be increased above the bulk value only once grain size becomes smaller than the coherence length (angstroms).²⁹ In this regime, the pair-breaking effect of the magnetic field is reduced, and H_{c2} enhancement results. The detailed shape of the $H_{c2}(T)$ curve will depend on the unknown distribution of grain sizes. At present, therefore, the individual contributions of each of these three mechanisms cannot be further assessed.

After having discussed the observed deviations from WHH, we reexamine more critically the assignment of T_0 as the superconducting critical temperature. Superconducting transition studies using ac susceptibility determine an irreversibility line, which is the same as the $H_{c2}(T)$ line for most superconductors. However, the reduction of the shielding volume fraction in high-dc magnetic fields (Figs. 1 and 2) suggests the presence of weak links that allow flux lines to move easily in response to an applied ac magnetic field. In the presence of flux motion on the time scale of the experiment (as observed in Ref. 5 for Rb_3C_{60}), the irreversibility line will equal the $H_{c2}(T)$ line only at the endpoints $H \rightarrow 0$ and $T \rightarrow 0$. At all intermediate values of the magnetic field, the irreversibility line will be shifted to lower temperatures by an amount that depends on the experimental drive frequency. Higher frequency allows less time for flux motion and thus provides a better approximation of the $H_{c2}(T)$ line. This effect can yield an observable frequency dependence of T_0 , as shown in Fig. 4 for two sets of data at $H = 12.5$ T. Note the shift of T_0 by ~ 0.3 K to higher temperatures as the drive frequency is increased by three orders of magnitude.

While flux motion and pinning barriers are difficult to characterize in detail, we can construct a simple model to estimate roughly T_c given the observed frequency dependence of T_0 . We then can present a range of WHH upper-critical-field curves (inset of Fig. 4), which are consistent with our low-field data including the effects of the

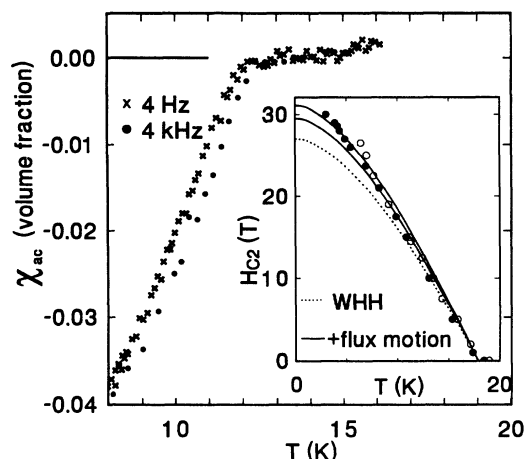


FIG. 4. Frequency dependence of the onset temperature, evidencing flux motion in K_3C_{60} powders. The crosses (circles) are data taken at 4 Hz (4 kHz). The inset contains the data and WHH curve from Fig. 3 (dotted line). The solid lines define a range of shifted WHH curves that are consistent with the observed flux motion.

observed flux motion. For this rough analysis, we assume a simple model of thermally activated flux motion over pinning barriers proportional to the condensation energy, i.e., proportional to $(T - T_c)$. We determine a range of

T_c values by varying the attempt frequency for flux motion from 10^9 s^{-1} to 10^{12} s^{-1} . Under these assumptions, T_c at $H = 12.5 \text{ T}$ would be $\sim 0.6\text{--}0.9 \text{ K}$ above the T_0 data of Fig. 3. The inset of Fig. 4 replots the Fig. 3 data and WHH curve (dotted line). The solid lines define a range of shifted WHH curves consistent with the observed flux motion. These shifted WHH curves keep T_c at $H = 0$ unchanged, yet increase T_c at $H = 12.5 \text{ T}$ by $0.6\text{--}0.9 \text{ K}$. It is clear that this simple model of flux motion can give reasonable agreement between WHH theory and our experimental results.

In conclusion, ac susceptibility measurements of superconducting K_3C_{60} powders in magnetic fields to 30 T yield a roughly linear $H_{c2}(T)$ curve with $-dH_{c2}/dT = 2.14 \pm 0.08 \text{ T/K}$. The observed H_{c2} at low temperatures exceed the $H_{c2}(T)$ curve from the standard theory by Werthamer-Helfand-Hohenberg. The deviations are likely due to flux motion in the K_3C_{60} powders, although further enhancement of $H_{c2}(0)$ by intrinsic mechanisms, such as strong coupling, Fermi-surface anisotropy, or sample granularity, may also play a role.

We thank E. Abrahams, R. C. Haddon, A. F. Hebard, D. A. Huse, A. P. Ramirez, M. A. Schluter, and J. Zaanen for assistance and valuable discussions. We also thank L. Rubin, S. Hannahs, and B. Brandt for support given at the Francis Bitter National Magnet Laboratory.

*On leave from P. N. Lebedev Physical Institute, Moscow, Russia.

¹A. F. Hebard, M. J. Rosseinsky, R. C. Haddon, D. W. Murphy, S. H. Glarum, T. T. M. Palstra, A. P. Ramirez, and A. R. Kortan, *Nature (London)* **350**, 600 (1991).

²K. Holczer, O. Klein, G. Gruner, J. D. Thompson, F. Diederich, and R. L. Whetten, *Phys. Rev. Lett.* **67**, 271 (1991).

³T. T. M. Palstra, R. C. Haddon, A. F. Hebard, and J. Zaanen, *Phys. Rev. Lett.* **68**, 1054 (1992).

⁴G. Sparn, J. D. Thompson, R. L. Whetten, S.-M. Huang, R. B. Kaner, F. Diederich, G. Gruner, and K. Holczer, *Phys. Rev. Lett.* **68**, 1228 (1992).

⁵C. Politis, B. Buntar, W. Krauss, and A. Gurevich, *Europhys. Lett.* **17**, 175 (1992).

⁶M. P. Gelfand and J. P. Lu, *Phys. Rev. Lett.* **68**, 1050 (1992); and (unpublished).

⁷O. V. Dolgov and I. I. Mazin, *Solid State Commun.* (to be published).

⁸S. C. Erwin and W. E. Pickett, *Science* **254**, 842 (1991).

⁹S. Satpathy, V. P. Antropov, O. K. Andersen, O. Jepsen, O. Gunnarsson, and A. I. Liechtenstein, *Phys. Rev. B* (to be published).

¹⁰M. Schluter, M. Lannoo, M. Needels, G. A. Baraff, and D. Tomanek, *Phys. Rev. Lett.* **68**, 526 (1992).

¹¹C. M. Varma, J. Zaanen, and K. Raghavachari, *Science* **254**, 989 (1991).

¹²S. J. Duclos, R. C. Haddon, S. H. Glarum, A. F. Hebard, and K. B. Lyons, *Science* **254**, 1625 (1991).

¹³I. I. Mazin, S. N. Rashkeev, V. P. Antropov, O. Jepsen, A. I. Liechtenstein, and O. K. Andersen, *Phys. Rev. B* **45**, 5114 (1992).

¹⁴K. Prassides, J. Tomkinson, C. Christides, M. J. Rosseinsky, D. W. Murphy, and R. C. Haddon, *Nature (London)* **354**, 462 (1991).

¹⁵P. W. Anderson (unpublished).

¹⁶S. Chakravarty, M. P. Gelfand, and S. Kivelson, *Science* **254**, 970 (1991).

¹⁷O. Gunnarsson and G. Zwicknagl (unpublished).

¹⁸M. Schluter *et al.*, *Phys. Rev. Lett.* **69**, 213 (1992).

¹⁹E. Helfand and N. R. Werthamer, *Phys. Rev.* **147**, 288 (1966); N. R. Werthamer, E. Helfand, and P. C. Hohenberg, *ibid.* **147**, 295 (1966).

²⁰F. Wudl, A. Hirsch, K. C. Khemani, T. Suzuki, P.-M. Allemand, A. Koch, H. Eckert, G. Srdanov, and H. M. Webb, *Am. Chem. Soc. Symp. Series* **481**, 161 (1992).

²¹R. Tycko, G. Dabbagh, M. J. Rosseinsky, D. W. Murphy, R. M. Fleming, A. P. Ramirez, and J. C. Tully, *Science* **253**, 884 (1991).

²²A. P. Ramirez (private communication).

²³S. H. Glarum, S. J. Duclos, and R. C. Haddon, *J. Am. Chem. Soc.* **114**, 1996 (1992).

²⁴R. Tycko, G. Dabbagh, M. J. Rosseinsky, D. W. Murphy, A. P. Ramirez, and R. M. Fleming, *Phys. Rev. Lett.* **68**, 1912 (1992).

²⁵Z. Zhang, C.-C. Chen, and C. M. Lieber, *Science* **254**, 1619 (1991).

²⁶J. P. Carbotte, *Rev. Mod. Phys.* **62**, 1027 (1990).

²⁷P. C. Hohenberg and N. R. Werthamer, *Phys. Rev. B* **153**, 493 (1967).

²⁸G. P. Kochanski, A. F. Hebard, R. C. Haddon, and A. T. Fiory, *Science* **255**, 184 (1992).

²⁹P. G. deGennes and M. Tinkham, *Physics* **1**, 107 (1964).